arXiv:cond-mat/0512652v1 [cond-mat.str-el] 26 Dec 2005

Thermodynamics of Spin-1/2 AF-AF-F and F-F-AF Trimerized Quantum Heisenberg Chains

Bo Gu and Gang Su*
College of Physical Sciences, Graduate University of Chinese Academy of Sciences, P. O. Box 4588, Beijing 100049, China

Song Gao
College of Chemistry and Molecular Engineering,
State Key Laboratory of Rare Earth Materials Chemistry and Applications, Peking University, Beijing 100871, China

The magnetization process, the susceptibility and the specific heat of the spin-1/2 AF-AF-F and F-F-AF trimerized quantum Heisenberg chains have been investigated by means of the transfer matrix renormalization group (TMRG) technique as well as the modified spin-wave (MSW) theory. A magnetization plateau at $m = 1/6$ for both trimerized chains is observed at low temperature. The susceptibility and the specific heat show various behaviors for different ferromagnetic and antiferromagnetic interactions and in different magnetic fields. The TMRG results of susceptibility and the specific heat can be nicely fitted by a linear superposition of double two-level systems, where two fitting equations are proposed. Three branch excitations, one gapless excitation and two gapful excitations, for both systems are found within the MSW theory. It is observed that the MSW theory captures the main characteristics of the thermodynamic behaviors at low temperatures. The TMRG results are also compared with the possible experimental data.

PACS numbers: 75.10.Jm, 75.40.Cx, 75.40.Mg

I. INTRODUCTION

Physical properties of low-dimensional magnetic materials have attracted considerable attention at the border of condensed matter physics. In particular, the bond-alternating quantum magnets with both ferromagnetic (F) and antiferromagnetic (AF) couplings have been extensively investigated, because they have exhibited quite fascinating properties owing to the competition of F and AF interactions. A simple AF bond-alternating chain (BAC) may be a F-AF alternating quantum Heisenberg chain, and the spin-1/2 copper-based compound $(IPA)CuCl_3$[1] is a typical example, in which the Haldane-like behavior has been observed. This kind of alternating chains have been actively studied both theoretically and experimentally in the last decades. Another interesting antiferromagnetic BAC is the F-F-AF alternating Heisenberg chain with period $n = 3$. According to Oshikawa-Yamanaka-Affleck (OYA)[2], the F-F-AF chain with spin S may exhibit a magnetization plateau at $m = S/3$, where m is the magnetization per site. In a typical example of spin-1/2 F-F-AF chain of $3CuCl_2 \cdot 2dx$ with strong F coupling (J_F) and weak AF coupling (J_{AF}), however, no plateau in the low-temperature magnetic curve has been observed[3]. Such a breakdown of the magnetization plateau in small bond ratio of $|J_{AF}/J_F|$[4] suggests that the OYA condition is only a necessary condition.

There is another intriguing BAC with period $n = 3$, which consists of AF-AF-F alternations, and is a ferrimagnet. The examples of AF-AF-F chains are $[Mn(L)_2(N_3)_2]_n$ with spin $S = 5/2$[5], $[M(4,4'bipy)(N_3)_2]_n$ with $M = Co$ ($S = 3/2$) and Ni ($S = 1$)[6], *and* $[Mn(N_3)_2(bpee)]_n$ *with* $S = 5/2$*[7].* These compounds have strong F and weak AF couplings, and no magnetization plateaus have been seen experimentally. If the ratio $|J_{AF}/J_F|$ are large enough, the plateaus could be expected during the magnetizing process. We note that the plateau has been observed experimentally in a F-F-AF-AF BAC compound, $Cu(3-Clpy)_2(N_3)_2$ [8, 9], which possesses a relatively large ratio $|J_{AF}/J_F|$ [10, 11].

Inspired by the exotic magnetic properties of the BAC compounds with period $n = 3$ observed experimentally, in this paper, we shall invoke the transfer matrix renormalization group (TMRG) technique [13] to study the thermodynamic properties of the AF-AF-F chain and F-F-AF chain, respectively. The rest of this paper is organized as follows. In Sec. II, we shall construct the model Hamiltonian for the trimerized J-J-J′ Heisenberg spin chain. In Sec. III, we shall present our TMRG results on the thermodynamic behaviors of the systems. The comparisons between the TMRG results and the results of the modified spin-wave (MSW) theory will be discussed in Sec. IV. Finally, a brief summary will be given.

II. MODEL

Let us consider a trimerized $S = 1/2$ J-J-J′ Heisenberg quantum spin chain. The Hamiltonian of the system reads

$$\begin{aligned} H &= \sum_j (J\mathbf{S}_{3j-2} \cdot \mathbf{S}_{3j-1} + J\mathbf{S}_{3j-1} \cdot \mathbf{S}_{3j} + J'\mathbf{S}_{3j} \cdot \mathbf{S}_{3j+1}) \\ &\quad -h \sum_j S_j^z, \end{aligned} \tag{1}$$

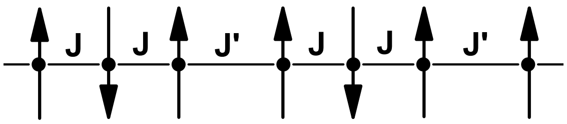

(a) AF-AF-F

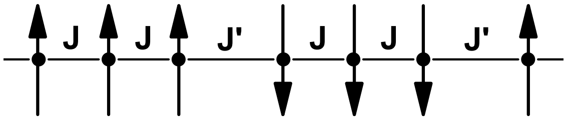

(b) F-F-AF

FIG. 1: Spin arrangements of the J-J-J′ trimerized spin chain with $S = 1/2$, where ↑ denotes spin up, ↓ denotes spin down, J and J' are exchange couplings. (a) AF-AF-F chain, $J = J_{AF}$, $J' = J_F$; (b) F-F-AF chain, $J = J_F$, $J' = J_{AF}$.

where J and J' are exchange integrals with J, $J' > 0$ denoting the antiferromagnetic coupling and J, $J' < 0$ the ferromagnetic coupling, h is the external magnetic field, and we take $g\mu_B = 1$. The schematic spin arrangements of the system are shown in Figs. 1. When $J = J' = J_F$ (or J_{AF}), the system becomes a uniform $S = 1/2$ Heisenberg ferromagnetic (or antiferromagnetic) chain.

When $J \neq J'$, as indicated in Figs. 1, if $J = J_{AF}$, $J' = J_F$, it is a ferrimagnetic spin chain (i.e. the configuration is AF-AF-F); if $J = J_F$, $J' = J_{AF}$, it becomes an antiferromagnetic system (i.e. the configuration is F-F-AF). The competition of F and AF couplings in these two trimerized chains would give rise to plenty of interesting characteristics. The magnetic properties of this model with S=1/2, 1, 3/2 and 2 in a magnetic field at zero temperature have been investigated by use of the density matrix renormalization group method[12]. It is purpose of this paper to study the thermodynamic properties of these trimerized quantum Heisenberg spin chains by means of the TMRG technique[13].

III. TMRG RESULTS

The TMRG method was detailed in two nice reviews[14], and we shall not repeat the technical skills here for concise. In our calculations, the number of kept optimal states is taken as $m = 64$ for the susceptibility χ, and $m = 80$ for the specific heat C, where the width of the imaginary time slice is taken as $\varepsilon = 0.1$. We have used different m and ε to verify the accuracy of calculations. At high temperature, the error caused by the Trotter-Suzuki decomposition is important and is of the order ε^3 for a fixed m. At low temperature, the error resulting from the basis truncation becomes important, which drops exponentially with increasing m initially and reaches to a finite value. The Trotter-Suzuki error is less than 10^{-3}, and the truncation error is smaller than 10^{-6} in our calculations. The physical quantities presented below are calculated down to $T = 0.025$ (in units of J_F).

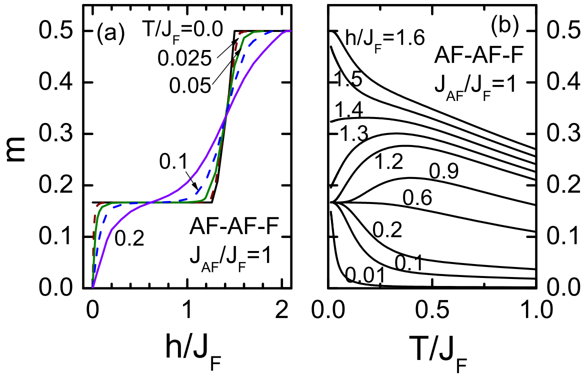

FIG. 2: (Color online) For the AF-AF-F chain with $J_{AF}/J_F = 1$: (a) The magnetization per site m as a function of magnetic field h at different temperatures; (b) The temperature dependence of m under different magnetic fields.

A. MAGNETIZATION

Fig. 2(a) shows the magnetization per site m as a function of magnetic field h at different temperatures for the AF-AF-F chain with $J_{AF}/J_F = 1$. At zero temperature, a magnetization plateau at $m = 1/6$ was observed[12]. As illustrated in Fig. 1(a), the ground state of the $S = 1/2$ AF-AF-F chain in the absence of the magnetic field corresponds to $m = 1/6$. When the external field is applied, the ground state with $m = 1/6$ still persists for $h/J_F < 1.3$, which is consistent with the OYA condition[2]. For $h/J_F > 1.3$ the plateau state is destructed, and $m(h)$ increases rapidly with increasing the field. When the field is increased to $h/J_F = 1.6$, $m(h)$ becomes saturated, and the ground state becomes a fully polarized state. When the temperature is increased, the magnetization plateau retains at low temperature, and is gradually smeared out at high temperature owing to the thermal fluctuations. It is noting that the magnetization $m(h)$ as a function of h at finite temperature starts from zero, that is nothing but the result of Mermin-Wagner theorem.

Fig. 2(b) gives the temperature dependence of the magnetization $m(T)$ under different magnetic fields for the AF-AF-F chain with $J_{AF}/J_F = 1$. It can be seen that $m(T)$ behaves distinctly for different ranges of the external field. At $h < 0.6$, $m(T)$ first decreases rapidly, and then declines slowly with increasing temperature; at

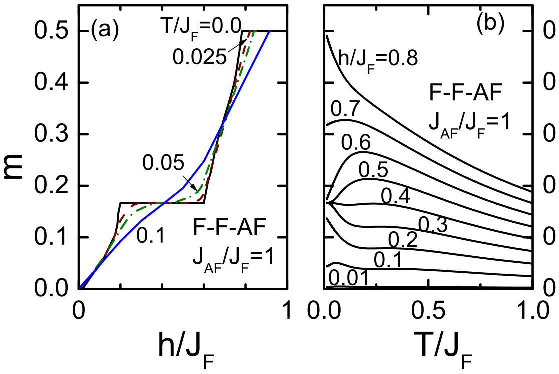

FIG. 3: (Color online) For the F-F-AF chain with $J_{AF}/J_F = 1$: (a) The magnetization per site m as a function of the magnetic field at different temperatures; (b) The temperature dependence of m under different fields.

$0.6 < h < 1.4$, $m(T)$ first increases, and then declines slowly with increasing temperature; at $h > 1.4$, $m(T)$ declines with increasing temperature. At $h = 0.6$ and 1.4, $m(T)$ appears to remain constant with zero curvature at low temperature, and declines slowly with temperature. It is found that just below and above $h = 0.6$ and 1.4, the curvature of $m(T)$ changes abruptly with opposite signs, implying that $h = 0.6$ and 1.4 could be viewed as the crossover fields. This observation is also consistent with Fig. 2(a) where there are two crossing points in the curves for different temperatures at $h = 0.6$ and 1.4.

Fig. 3(a) shows the field dependence of the magnetization per site $m(h)$ at different temperatures for the F-F-AF chain with $J_{AF}/J_F = 1$. A magnetization plateau at $m = 1/6$ is also observed at zero temperature. As indicated in Fig. 1(b), the ground state of the $S = 1/2$ AF-AF-F chain in the absence of a magnetic field corresponds to $m = 0$. With increasing the magnetic field, m first increases till to $m = 1/6$ at $h/J_F \approx 0.2$, then goes into the plateau state with $m = 1/6$ for $h/J_F < 0.7$, beyond which the plateau state is destroyed, and $m(h)$ then increases rapidly to a saturation at $h/J_F = 0.8$ where the system becomes fully polarized. The occurrence of the plateau state with $m = 1/6$ is also consistent with the OYA condition[2]. It is seen that at low temperature the magnetization plateau still persists, though the width of plateau is getting narrow. At high temperature, the plateau is gradually smeared out by thermal fluctuations, and m(h) increases nonmonotonically till the saturation with increasing the magnetic field.

The temperature dependence of the magnetization per site $m(T)$ under different fields for the F-F-AF chain with $J_{AF}/J_F = 1$ is presented in Fig. 3(b). One may see that $m(T)$ shows different behaviors at low temperature in different ranges of the magnetic field. At $h < 0.2$, $m(T)$ increases first and then declines smoothly with increasing temperature; at $0.2 < h < 0.4$, $m(T)$ decreases dramatically at low temperature and then slowly with increasing temperature; at $0.4 < h < 0.7$, $m(T)$ increases at low temperature and then declines slowly with increasing temperature; at $h > 0.7$, $m(T)$ declines remarkably with increasing temperature. At $h = 0.4$ and 0.7, $m(T)$ remains almost unchanged at lower temperature, and then declines slowly with increasing T. Again, the curvature of $m(T)$ changes abruptly with opposite signs just below and above $h = 0.4$ and 0.7. The results presented in Fig. 3(b) suggest that at low temperature the system may enter into different states in different ranges of the magnetic field, namely, for $h < 0.2$, the system is in an ordering state; for $0.2 < h < 0.4$ the system could go into the spin-canting state; for $0.4 < h < 0.7$ the system enters into the plateau state where the excitations are gapful; and for $h > 0.7$ the system goes into another ordering state before saturation.

It is interesting to note that the magnetization as a function of magnetic field and temperature exhibits different behaviors for the AF-AF-F chain and the F-F-AF chain, for the former is a ferrimagnet, while the latter is an antiferromagnet. However, both systems shows a magnetization plateau with $m = 1/6$ at low temperature, being in agreement with the OYA condition.

B. SUSCEPTIBILITY

Let us now present the TMRG results of the susceptibility (χ) as a function of temperature (T) for the AF-AF-F chain. In the absence of the magnetic field, the susceptibility diverges when the temperature tends to zero, and with increasing temperature, χ decreases rapidly, as shown in Fig. 4(a). For different J_{AF}/J_F, $\chi(T)$ exhibits similar behaviors at low T, but distinct behaviors at moderate T, as manifested in the inset of Fig. 4(a), where χT versus T is plotted for various J_{AF}/J_F, and a low-T divergence and a round minimum are observed for $J_{AF}/J_F \leq 1$, indicating that when the F interaction J_F predominates, the system shows a ferrimagnetic behavior; when the AF interaction J_{AF} is predominant, the system falls into a trimerized bond state. In the presence of the magnetic field, the susceptibility χ shows quite different behaviors, as presented in Figs. 4(b) and (c) at $J_{AF}/J_F = 1$. Unlike the case of $h = 0$, χ under nonzero h exhibits a peak at low temperature except $h = 0.6$ and 1.4 where with increasing T, χ first increases and then drops slowly for the former, and goes to divergence at low temperature for the latter. With the increase of h, the peak of χ appears to become rounded, and the peak height of χ gets suppressed for $h < 0.6$, then increased for $0.6 < h < 1.4$, and then becomes suppressed again for $h > 1.4$. These observations show again that the system can enter into different states within different ranges of the magnetic field.

For the F-F-AF chain, the temperature dependence

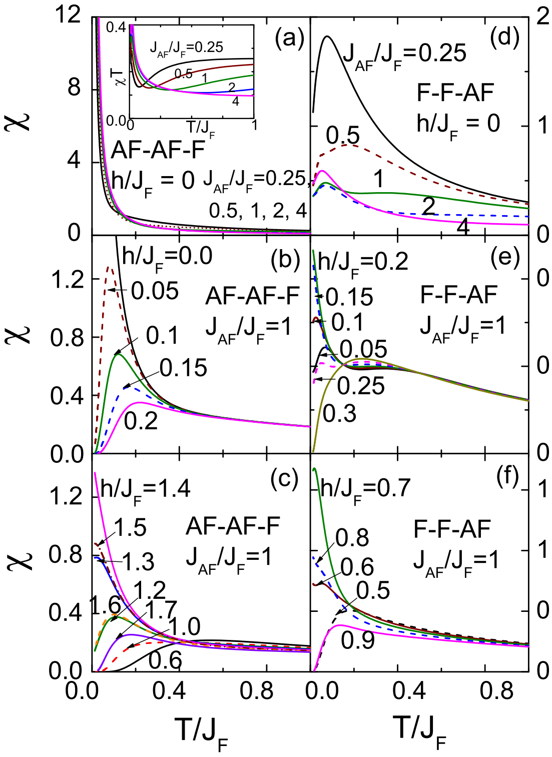

FIG. 4: (Color online) The temperature dependence of the susceptibility χ. For the AF-AF-F chain (a) at $h = 0$ for different J_{AF}/J_F, (b) and (c) at $J_{AF}/J_F = 1$ for different external fields, where the inset of (a) depicts χT against T for different J_{AF}/J_F. For the F-F-AF chain (d) at $h = 0$ for different J_{AF}/J_F, (e) and (f) at $J_{AF}/J_F = 1$ for different external fields.

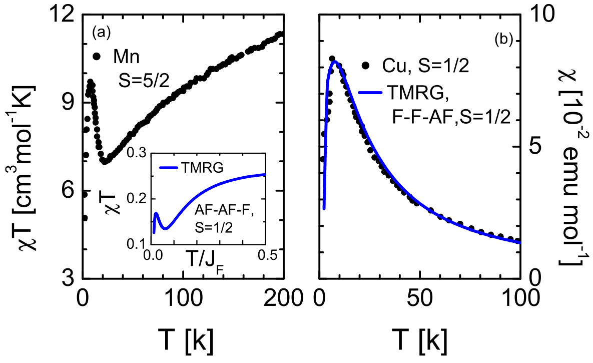

FIG. 5: (Color online) (a) The experimental data of χT of the spin-5/2 AF-AF-F chain $[Mn_3(N_3)_6(bpe)_3]$ (from Ref.[7]); Inset presents the TMRG result of an AF-AF-F chain with $S = 1/2$. (b) A comparison of the susceptibility for $3CuCl_2 \cdot 2dx$ with the TMRG result of a F-F-AF chain with $S = 1/2$, where the experimental data are taken from Ref. [3].

of the susceptibility χ for different J_{AF}/J_F and h is shown in Figs. 4(d)-(f), respectively. In the absence of the magnetic field, the susceptibility reveals peaks at low temperature for different J_{AF}/J_F, and $\chi = 0$ at $T = 0$. When J_{AF}/J_F is either smaller or larger, e.g., $J_{AF}/J_F = 0.25$, 2, 4, χ shows one peak; while $J_{AF}/J_F = 0.5$ and 1, χ shows a double-peak structure, as manifested in Fig. 4(d). The calculated results indicate that the system shows an AF behavior. It seems that the double-peak structure comes from the two different kinds of excitations induced by the competition between F and AF interactions. In the presence of the magnetic field, the temperature dependence of the susceptibility χ at $J_{AF}/J_F = 1$ for different external fields are presented in Figs. 4(e) and (f). It is found that $\chi(T)$ behaves variously in different ranges of the magnetic field. When h is small, $\chi(T)$ shows a double-peak structure at low temperature with the first peak sharp and the second peak round; with increasing h, the height of the first peak grows dramatically, while that of the second round peak leaves almost unchanged; when $h/J_F > 0.2$, the first peak is remarkably suppressed at $h/J_F = 0.25$, and vanishes at $h/J_F = 0.3$, while the second round peak becomes slightly higher, as shown in Fig. 4(e). When $h/J_F > 0.5$, the second peak of χ moves to the low-temperature side, and at $h/J_F = 0.7$, the two peaks merge into a single; when h is increased further, the peak of χ is suppressed again. The behaviors of $\chi(T)$ show that the F-F-AF chain can enter into different states at low temperatures under different magnetic fields, consistent with the results presented in Fig. 3(b).

To verify our TMRG results, we have included the experimental data of an AF-AF-F chain compound $[Mn_3(N_3)_6(bpe)_3]$ and a F-F-AF chain compound $3CuCl_2 \cdot 2dx$ in Figs. 5 for a comparison. Fig. 5(a) shows the experimental data of χT versus T for $[Mn_3(N_3)_6(bpe)_3]$, whose magnetic structure is an AF-AF-F chain with spin-5/2 [7]. Owing to our computing capacity, we cannot at present calculate directly the magnetic properties of the spin-5/2 AF-AF-F chain by using the TMRG method. As a qualitative understanding, however, in the inset of Fig. 5(a), we have presented our TMRG result of a spin-1/2 AF-AF-F chain with $h/J_F = 0.003$ and $J_{AF}/J_F = 0.2$. It can be seen that the experimental and calculated curves share qualitatively similar characteristics. Fig. 5(b) gives a comparison of the experimental susceptibility of the compound $3CuCl_2 \cdot 2dx$, which is a F-F-AF chain with spin-1/2 [3], with the TMRG result. It is found that our TMRG result fits well with the experimental data, with the coupling parameters $J_{AF}/J_F = 0.2$, $J_F = 100$ K, and $h/J_F = 0.005$. Our calculated result is in agreement with the previous theoretical result[3].

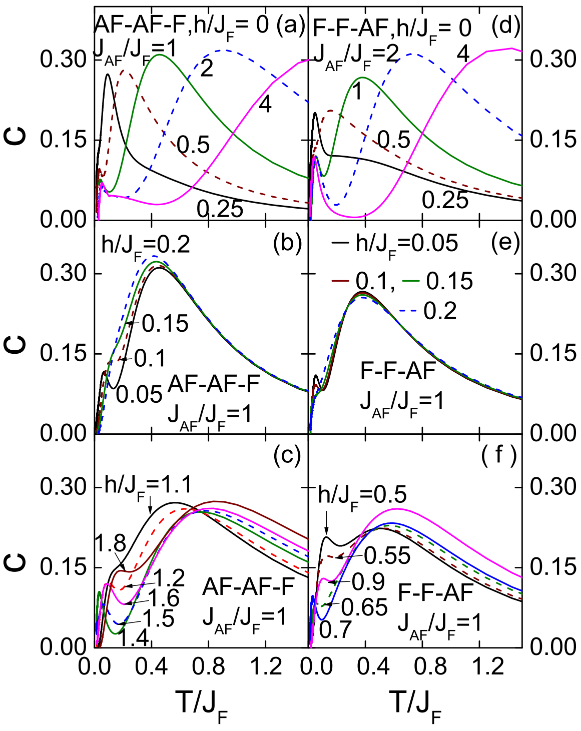

FIG. 6: (Color online) The temperature dependence of the specific heat C. For the AF-AF-F chain (a) at $h = 0$ for different J_{AF}/J_F, (b) and (c) at $J_{AF}/J_F = 1$ for different external fields. For the F-F-AF chain (d) at $h = 0$ for different J_{AF}/J_F, (e) and (f) at $J_{AF}/J_F = 1$ for different external fields.

C. SPECIFIC HEAT

In this subsection, we shall discuss the specific heat of the spin-1/2 AF-AF-F and F-F-AF chains, as shown in Figs. 6 for different J_{AF}/J_F and h. For the AF-AF-F chain, in absence of the magnetic field, the specific heat C as a function of temperature shows clearly a double-peak structure, as indicated in Fig. 6(a). With increasing J_{AF}/J_F, the low-temperature peak of C leaves almost unchanged, while the second peak moves to the high-temperature side, and gets rounded. This feature of the specific heat shows that the system might exist two different kinds of excitations due to the competition of F and AF interactions, as will be discussed in next section. It seems that the first peak corresponds to the F excitations, while the second peak corresponds to the AF excitations.

In presence of the magnetic field, the temperature dependence of the specific heat C for the AF-AF-F chain with $J_{AF}/J_F = 1$ is shown in Figs. 6(b) and (c) under different fields. When h is small, the double-peak structure of C is observed; with increasing h, the first peak tends to vanish, while the second peak remains almost unchanged, as shown in Fig. 6(b). When $0.2 < h/J_F < 1.1$, the two peaks become a single. When $h/J_F > 1.1$, as presented in Fig. 6(c), the first peak recovers anew, and with the increase of h, the first peak moves to the lower temperature side till $h/J_F = 1.4$, then shifts to the high temperature side for $1.8 > h/J_F > 1.4$, and tends to vanish for $h/J_F > 1.8$, while the second peak shifts slightly to the higher temperature side with increasing h. The results show that the system is in a few different states under different magnetic fields.

For the F-F-AF chain, the temperature dependence of the specific heat C is shown in Figs. 6(d)-(f) for different J_{AF}/J_F and h. In absence of the magnetic field, C also shows a double-peak structure; with increasing J_{AF}/J_F, the height of the first peak of C is suppressed but its position leaves unchanged, while the second peak tends to shift to the high-temperature side, as illustrated in Fig. 6(d). It is seen that the qualitative behavior is similar to that of the AF-AF-F chain presented in Fig. 6(a). The results suggest that the F-F-AF chain has also two kinds of excitations due to the competition of F and AF interactions.

Figs. 6(e) and (f) gives the temperature dependence of the specific heat C for the F-F-AF chain with $J_{AF}/J_F = 1$ under different magnetic fields. Similar to the AF-AF-F chain, with increasing h, the first peak of C is gradually suppressed, while the second peak retains nearly intact till $h/J_F = 0.2$. When $0.2 < h/J_F < 0.5$, the first peak is completely suppressed; when $0.5 < h/J_F < 0.7$, with the increase of h, the first peak recovers again with the peak height decreased and the peak position shifted to the lower temperature side, while the second peak moves slightly to the high temperature side with the peak height a little bit enhanced; when $h/J_F > 0.7$, the situation changes, namely, with increasing h, the first peak of C is enhanced and moves to the high temperature side, and the second peak is also promoted. The present observation displays that the F-F-AF chain falls into different thermodynamic states under different external fields, and has some behaviors similar to the AF-AF-F chain, although both chains have quite different ground states, as the latter is a ferrimagnet, while the former is an antiferromagnet.

D. FITTING TO A SUPERPOSITION OF DOUBLE TWO-LEVEL SYSTEMS

The double-peak structure of the temperature dependence of the specific heat can be viewed as a minimum at low temperature and a Schottky-like maximum at high temperature. The Schottky-like anomaly can be fitted with a so-called two-level system, where the thermal population of the levels is governed by the Maxwell-Bolzman statistics, $n_i = e^{-\varepsilon_i/k_BT}/Z$ $(i = 1, 2)$ with the distribution function $Z = e^{-\varepsilon_1/k_BT} + e^{-\varepsilon_2/k_BT}$, and the total energy $E(T) = n_1\varepsilon_1 + n_2\varepsilon_2$. The specific heat can be obtained by $C = (\partial E/\partial T)$. Define $\varepsilon_1 = 0$, $\varepsilon_2 = \Delta$. The

Schottky-like specific heat can be written as

$$C_s(\Delta,T)=k_B(\frac{\Delta}{k_BT})^2\frac{e^{\Delta/k_BT}}{(1+e^{\Delta/k_BT})^2}. \qquad (2)$$

Similarly, it is found that the magnetic susceptibility can be fitted by[15],

$$\chi_s(\Delta,T)=k_B(\frac{\Delta}{k_BT})\frac{e^{\Delta/k_BT}}{(1+e^{\Delta/k_BT})^2}, \qquad (3)$$

where Δ is the excitation gap. However, our TMRG results cannot be well fitted by these above two formulae. By noting that the present systems such as the AF-AF-F and F-F-AF chains are quantum trimerized systems with a period $n=3$, and the double-peak structure may be regarded as the consequence of the competition between F and AF excitations, the thermodynamic properties of these systems could be mimicked by a superposition of double two-level systems. As a result, the susceptibility for the AF-AF-F and F-F-AF chains may be expected to fit by

$$\chi(T)=A_1\chi_s(\Delta_1,T)+A_2\chi_s(\Delta_2,T), \qquad (4)$$

and the double-peak structure of the specific heat can be fitted by the following form:

$$C(T)=A_1C_s(\Delta_1,T)+A_2C_s(\Delta_2,T), \qquad (5)$$

where A_1, A_2 are fitting parameters, and Δ_1, Δ_2 are the excitation gaps for the double two-level systems. In these above equations, χ_s and C_s are defined by Eqs. (3) and (2), respectively.

For the AF-AF-F chain, in absence of the magnetic field, we have found that $\chi(T)$ cannot be fitted by Eq. (4), but can be well fitted by the equation $\chi(T)=a(T/J_F)^{-2}-b(T/J_F)^{-3/2}+c(T/J_F)^{-1}$ with a, b, and c the fitting parameters, as shown in Fig. 7(a) for $J_{AF}/J_F=0.5$ as an example. We note that the susceptibility of a spin-1/2 ferromagnetic system was expanded as $\chi J/L(g\mu_B)^2=0.04167t^{-2}-0.145t^{-1.5}+0.17t^{-1}+O(t^{-0.5})$ with $t=-k_BT/J$ $(J<0)$ at low temperatures[16]. Thus, it is not surprising that the present system shows a similar behavior, as the AF-AF-F chain is a ferrimagnet. However, in presence of the magnetic field, the susceptibility $\chi(T)$ of the AF-AF-F chain can be nicely fitted by Eq. (4), as compared in Fig. 7(b) for $J_{AF}/J_F=1$ and $h/J_F=1.7$ as an example. Figs. 7(c) and (d) give the TMRG fitting results in terms of Eq. (4) for the susceptibility $\chi(T)$ of the F-F-AF chain in absence and presence of the magnetic field, respectively. One may see that apart from the case where $\chi(T)$ is divergent at lower temperature and cannot be fitted by Eq. (4), the susceptibility as a function of temperature for both trimerized chains can be well fitted by a superposition of the double two-level systems.

Figs. 8 present the TMRG results of the specific heat as a function of temperature fitting to a superposition of double two-level systems characterized by Eq. (5) for

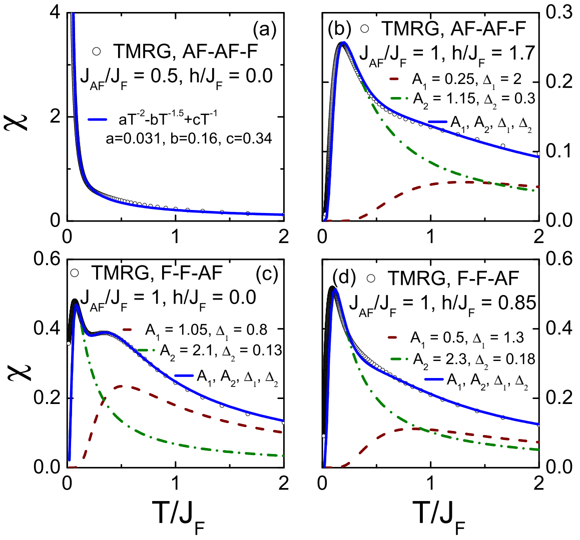

FIG. 7: (Color online) The TMRG results of the susceptibility as a function of temperature are fitted. For the AF-AF-F chain (a) by $a(T/J_F)^{-2}-b(T/J_F)^{-3/2}+c(T/J_F)^{-1}$ for $h=0$, (b) by Eq. (4) for h nonzero; for the F-F-AF chain by Eq. (4) for (c) $h=0$, and (d) h nonzero.

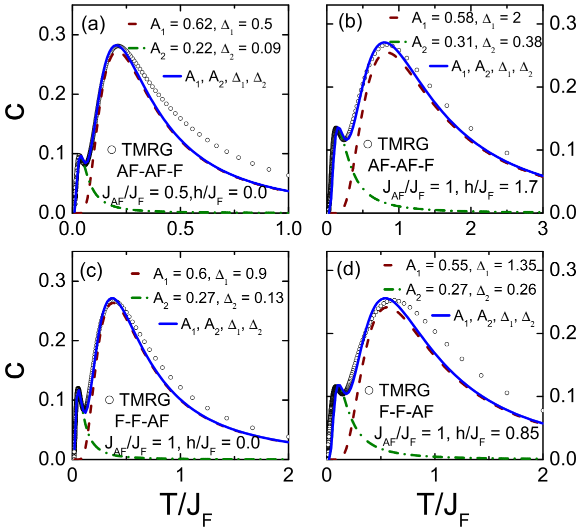

FIG. 8: (Color online) The TMRG results of the specific heat as a function of temperature are fitted by Eq. (5). For the AF-AF-F chain with (a) $J_{AF}/J_F=0.5$ and $h=0$, and (b) $J_{AF}/J_F=1.7$ and $h/J_F=1.7$; for the F-F-AF chain with $J_{AF}/J_F=1$ and (c) $h=0$ and (d) $h/J_F=0.85$.

the AF-AF-F and F-F-AF chains. It can be found that the specific heat with double-peak structure can be well fitted by Eq. (5) at low temperature, with only a slightly quantitative deviation at high temperature, showing that the main features of the specific heat of both trimerized chains can be reproduced by a superposition of double two-level systems. The fitting results could give the two excitation gaps. The reasons for such nice fittings come from the fact that these two trimerized chains have three branches of excitations (see next section), one gapless F excitations, and two gapful excitations, which could be equivalently treated by a superposition of double two-level systems with two gaps Δ_1 and Δ_2. We have also found that a direct fitting to a three-level system is not as good as to double two-level systems.

IV. MODIFIED SPIN-WAVE THEORY

The zero-field specific heat of a quantum ferrimagnet, which is believed as an intrinsic double-peak structure of topological origin and is different from the external field induced double-peak structure, was investigated by using the modified spin-wave (MSW) theory[17, 18, 19], where it has been found that in the case of the AF-AF-F-F BAC, there are four distinct branches of spin-wave excitations, say, the lower two ferromagnetic bands construct the low-temperature bump, while an upper ferromagnetic band and an antiferromagnetic band contribute to a Schottky-type peak at mid temperatures.

The field-induced double-peak structure of the specific heat in a quantum ferrimagnet has also been studied by using the linear spin-wave theory[20]. In the case of spin-$(1, \frac{1}{2})$ ferrimagnet, a simple picture was given by noting that the Zeeman term introduces a gap to the F excitations that increases with increasing the field, and a gap to the AF excitations that decreases with increasing the field, and the specific heat really reflects the dual structure of the antiferromagnetic and ferromagnetic excitations for all fields.

The MSW theory can also be applied to the present $S = 1/2$ AF-AF-F and F-F-AF chains in absence of the external field so that our TMRG results of the thermodynamic quantities may be used to compare with the corresponding MSW results. In the conventional spin-wave scheme, the spin deviations in each sublattice diverge in the one-dimensional (1D) antiferromagnets, but the quantum as well as thermal divergence of the number of bosons can be overcome in the Takahashi scheme[17] that will be applied to the present antiferromagnetic F-F-AF chain. The AF-AF-F chain is a ferrimagnet, whose magnetization should be nonzero in the ground state but zero at finite temperature, leading to that we can apply the Yamamoto scheme[21, 22], where the Lagrange multiplier was introduced directly in the free energy, to our present ferrimagnetic AF-AF-F chain. The detail derivations of the MSW formalism are collected in Appendix A, where the linear modified spin-wave (LMSW) theory, which is up to the order of $O(S^1)$, and the perturbational interacting modified spin-wave (PIMSW) theory, which is up to the order of $O(S^0)$, are included. Our results show that the MSW results may describe well the low-temperature behavior of the system, but they are not good in agreement with the TMRG results at high temperature.

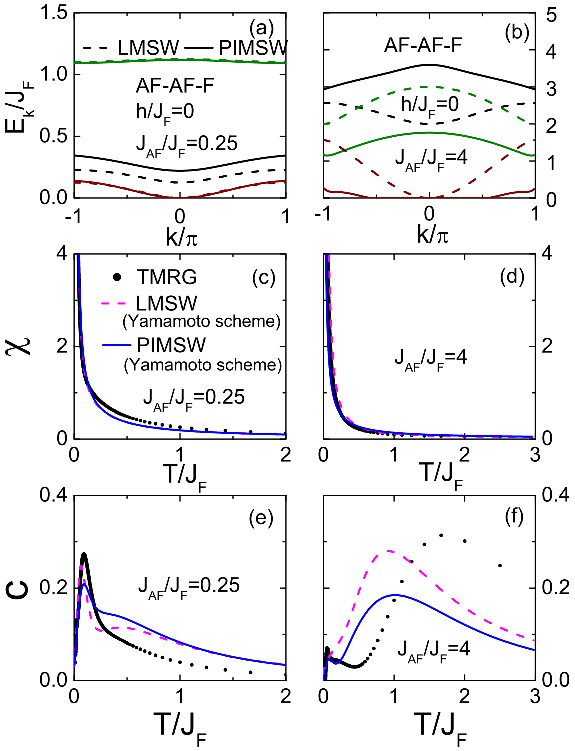

FIG. 9: (Color online) The excitation spectra of the AF-AF-F chain calculated by the LMSW and PIMSW methods with (a) $J_{AF}/J_F = 0.25$ and (b) $J_{AF}/J_F = 4$. A comparison of the TMRG results with the LMSW and PIMSW results of the susceptibility $\chi(T)$ for the AF-AF-F chain with (c) $J_{AF}/J_F = 0.25$ and (d) $J_{AF}/J_F = 4$. The comparison of TMRG with LMSW and PIMSW results of the specific heat $C(T)$ for the AF-AF-F chain with (e) $J_{AF}/J_F = 0.25$ and (f) $J_{AF}/J_F = 4$.

Figs. 9(a) and (b) present the zero-field excitation spectra which were calculated by the LMSW and PIMSW methods within the Yamamoto scheme for the AF-AF-F chain. It is seen that this trimerized system has three branches of excitation spectra, one gapless excitation spectrum and two gapful excitation spectra. When J_{AF}/J_F is small, the lower F gapless spectrum and the upper AF gapful spectrum look coincidence, while the mid F branches are slightly shifted; when J_{AF}/J_F becomes large, the lower F branch is far separated from the mid and upper excitation spectra for the PIMSW results, while for the LMSW results, the excitation spectra are more dispersive, and the mid branch has two crossing points with the upper branch, showing that the LMSW and PIMSW methods give different results when the AF interaction is more dominant. Figs. 9(c) and (d) show the comparison between the TMRG and LMSW and PIMSW results of the temperature dependence of the zero-field susceptibility for the AF-AF-F chain with different J_{AF}/J_F. When J_{AF}/J_F is large, the LMSW and PIMSW results of $\chi(T)$ are in agreement with the TMRG result, as shown in Figs. 9(d); when J_{AF}/J_F is small, say, the F interaction takes predominant, the low-temperature behavior of $\chi(T)$ calculated by the LMSW and PIMSW theories coincides with the TMRG result, while the high-temperature behavior shows a somewhat difference, as shown Figs. 9(c). Figs. 9(e) and (f) give the comparison of the LMSW and PIMSW results with the TMRG result of the zero-field specific heat $C(T)$ for the AF-AF-F chain with different J_{AF}/J_F. It can be seen that the LMSW and PIMSW theories can be applied to describe the specific heat of the AF-AF-F chain at lower temperature, where the PIMSW result can fairly recover the first peak position of $C(T)$ at lower temperature, but they cannot describe well the high-temperature behavior where both MSW results look only qualitatively similar to the TMRG result. However, it can be stated that the double-peak structure of the specific heat is intimately related to the three branch excitations of the trimerized system, as manifested by the MSW results.

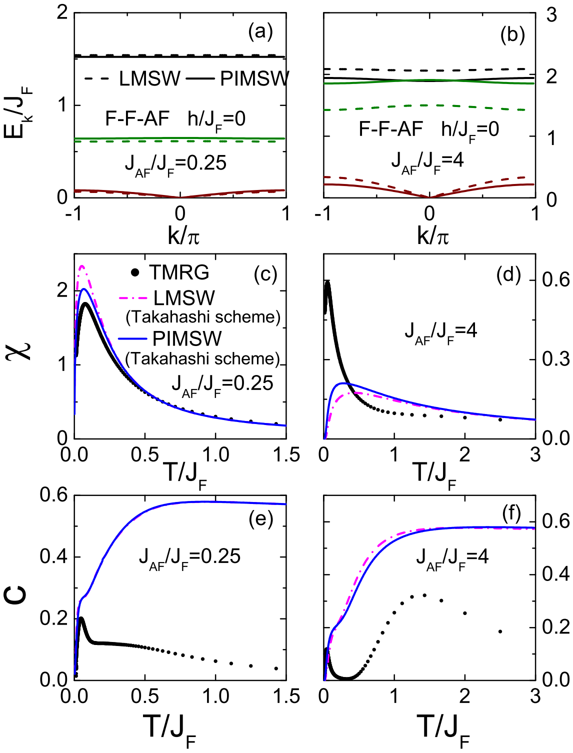

FIG. 10: (Color online) The excitation spectra of the F-F-AF chain calculated by the LMSW and PIMSW methods with (a) $J_{AF}/J_F = 0.25$ and (b) $J_{AF}/J_F = 4$. A comparison of the TMRG results with the LMSW and PIMSW results of the susceptibility $\chi(T)$ for the F-F-AF chain with (c) $J_{AF}/J_F = 0.25$ and (d) $J_{AF}/J_F = 4$. The comparison of TMRG with LMSW and PIMSW results of the specific heat $C(T)$ for the F-F-AF chain with (e) $J_{AF}/J_F = 0.25$ and (f) $J_{AF}/J_F = 4$.

Figs. 10(a) and (b) present the excitation spectra calculated by the LMSW and PIMSW methods within the Takahashi scheme for the F-F-AF chain with $J_{AF}/J_F = 0.25$ and 4 in absence of the magnetic field, respectively. There are also three branch excitations, i.e., one F gapless excitation spectrum, and two gapful excitation spectra, which are responsible for the thermodynamic behaviors of the system at low temperature. When the AF interaction is weak, the LMSW and PIMSW theories give a similar result, as shown in Fig. 10(a); when the AF interaction becomes stronger, both methods produce quite different results particularly for the upper excitation branches, say, the two upper excitation spectra calculated from the PIMSW method have two crossings, while those calculated by the LMSW method are separated, as indicated in Fig. 10(b), showing that the LMSW and PIMSW methods should be cautiously applied when the F interaction of the system is weaker. Figs. 10(c) and (d) show a comparison between the TMRG and MSW results of the temperature dependence of the zero-field susceptibility for the F-F-AF chain with $J_{AF}/J_F = 0.25$ and 4, respectively. One may see that when J_{AF}/J_F is small, the low-temperature peak of $\chi(T)$ can be fairly recovered, although there are somewhat differences; when J_{AF}/J_F is large, say, the F interaction is weak, the position of low-temperature peak of $\chi(T)$ can be clearly reproduced, although there are quantitative changes, indicating that the LMSW and PIMSW methods could capture the main characteristics of the low-lying excitations of the present trimerized system at low temperature. Figs. 10(e) and (f) give the comparison between the TMRG and MSW results of the zero-field specific heat $C(T)$ for the F-F-AF chain with $J_{AF}/J_F = 0.25$ and 4, respectively. It is seen that the double-peak structure of $C(T)$ can also be obtained by the LSMSW and PIMSW methods, which can produce the main features of the specific heat of the system at low temperature, but have large deviations at high temperature.

V. SUMMARY

In this paper, we have numerically studied the thermodynamics of the $S = 1/2$ AF-AF-F and F-F-AF trimerized quantum Heisenberg chains by means of the TMRG method and the MSW theory. The magnetization process, the low-lying excitations, the susceptibility and the specific heat of both systems have been explored. It is found that the TMRG results of the temperature dependence of the susceptibility as well as the specific heat can be nicely fitted by a superposition of double two-level systems, and two fitting equations for the peak structures are proposed. For the AF-AF-F chain with strong F interactions, $\chi(T)$ can be well fitted by a polynomial.

For the AF-AF-F chain which is a ferrimagnet, it is observed that the magnetic curve $m(h)$ reveals some peculiar behaviors where a magnetization plateau at $m = 1/6$ is observed at low temperature T, while the plateau is smeared out when T is increased, and the temperature dependence of the magnetization $m(T)$ shows various behaviors in different ranges of the magnetic field. The susceptibility $\chi(T)$ exhibits different behaviors in different fields: at $h = 0$, $\chi(T)$ goes to divergent at lower T and decreases with increasing T for $J_{AF}/J_F \leq 1$; at $h \neq 0$, $\chi(T)$ shows a low-temperature peak for $J_{AF}/J_F = 1$ except $h/J_F = 0.6$ and 1.4, and decreases at high T, where the peak height and position of $\chi(T)$ vary under different h. The behavior of χT against T for a spin-5/2 AF-AF-F chain compound $[Mn_3(N_3)_6(bpe)_3]$ looks qualitatively similar to the TMRG result of a spin-1/2 AF-AF-F chain. The specific heat $C(T)$ is found to show a double-peak structure, with the peak height and position varying for different J_{AF}/J_F as well as under different h. The results of $m(T)$, $\chi(T)$ and $C(T)$ show that the system under interest could be in several different states under different magnetic fields.

For the F-F-AF chain which is an antiferromagnet, it is found that the magnetization process shows an interesting behavior, and a magnetization plateau at $m = 1/6$ is also seen at low temperature which is smeared out at high temperature. $m(T)$ displays different behaviors in different regimes of the magnetic field, which is further confirmed by the TMRG results of the susceptibility $\chi(T)$ where a peak is observed at low temperature, but the peak height and position are found dependent on different ranges of h. The experimental data of $\chi(T)$ for the spin-1/2 F-F-AF chain compound $3CuCl_2 \cdot 2dx$ is compared with the corresponding TMRG result, which is found quite agreement. The specific heat as a function of temperature shows a double-peak structure, whose shapes change with different J_{AF}/J_F as well as in different magnetic fields.

The MSW theory within the Yamamoto scheme as well as the Takahashi scheme is also applied to study the thermodynamics of the present trimerized quantum Heisenberg AF-AF-F chain and F-F-AF chain, respectively. Three branch excitations are found for both systems, say, one gapless excitation spectrum and two gapful excitation spectra, that come from the competition between the F and AF interactions. A perfect fitting of $\chi(T)$ and $C(T)$ to a superposition of double two-level systems could be reasonably understood within the framework of the MSW theory. It is three branch excitations with two gaps in the long wave-length limit that are responsible for the peak structures of the susceptibility and the specific heat observed by the TMRG calculations. It is found that the MSW theory could to some extent describe the low-temperature behavior of the systems, and gives only a qualitative description for $\chi(T)$ and $C(T)$ of AF-AF-F chain and $\chi(T)$ of F-F-AF chain at high temperature, but has a large deviation for $C(T)$ of the F-F-AF chain at high temperature.

Finally, we would like to state that the present TMRG and MSW results could be helpful for understanding the magnetization process as well as the thermodynamic properties of the AF-AF-F and F-F-AF trimerized quantum spin chains. As there are few experimental data available for such systems at present, we expect that more experiments can be performed in near future to verify our theoretical findings.

APPENDIX A: MSW THEORY FOR THE TRIMERIZED F-F-AF CHAIN

The formalism of the MSW theory for the AF-AF-F chain can be found in Ref. [23]. In this Appendix, the MSW theory for the F-F-AF chain is formulated. The Hamiltonian of the 1D spin-1/2 F-F-AF chain can be written as

$$\begin{aligned} H &= \sum_{n=1}^{N}(J_F\mathbf{S}_{1n}\cdot\mathbf{S}_{2n} + J_F\mathbf{S}_{2n}\cdot\mathbf{S}_{3n} + J_{AF}\mathbf{S}_{3n}\cdot\mathbf{S}_{4n} \\ &\quad J_F\mathbf{S}_{4n}\cdot\mathbf{S}_{5n} + J_F\mathbf{S}_{5n}\cdot\mathbf{S}_{6n} + J_{AF}\mathbf{S}_{6n}\cdot\mathbf{S}_{1n+1}), \end{aligned}$$

where $6N$ is the length of the F-F-AF chain and $J_F < 0$, $J_{AF} > 0$. We start from the Holstein-Primakoff (HP) transformation

$$\begin{aligned} S_{in}^{+} &= \sqrt{2S - a_{in}^{+}a_{in}}\,a_{in}, \\ S_{in}^{z} &= S - a_{in}^{+}a_{in}, \\ S_{jn}^{+} &= a_{jn}^{+}\sqrt{2S - a_{jn}^{+}a_{jn}}, \\ S_{jn}^{z} &= -S + a_{jn}^{+}a_{jn}, \end{aligned} \tag{A1}$$

where $S = 1/2$, $i = 1$, 2, 3 and $j = 4$, 5, 6. The LMSW method treats the HP transformation up to $\mathrm{O}(S^1)$, while the PIMSW method treats is the HP transformation up to $\mathrm{O}(S^0)$ where the interactions between spin waves are handled perturbatively.

In the conventional spin-wave scheme, the spin deviations in each sublattice, $\langle a_{ik}^{+}a_{ik}\rangle$, diverge in the antiferromagnetic ground state but stay finite in the ferrimagnetic ground state. In the AF system, the quantum as well as the thermal divergences of the number of bosons are all suppressed:

$$\begin{aligned} 0 &= \sum_{n}\langle S_{1n}^{z} + S_{2n}^{z} + S_{3n}^{z} - S_{4n}^{z} - S_{5n}^{z} - S_{6n}^{z}\rangle \\ &= 6NS - \sum_{k}\sum_{i=1}^{6}\langle a_{ik}^{+}a_{ik}\rangle. \end{aligned} \tag{A2}$$

As the F-F-AF is an antiferromagnet, the Takahashi scheme[17] will be invoked. In order to enforce the constraint (A2), a Lagrange multiplier μ is introduced to the

Hamiltonian

$$\tilde{H} = H + \mu \sum_k \sum_{i=1}^{6} a_{ik}^{+} a_{ik}.$$

The Fourier transformations are defined by

$$\begin{aligned} a_{ln} &= \frac{1}{\sqrt{N}} \sum_k e^{ik(n-7/12+l/6)} a_{lk}, \\ a_{mn} &= \frac{1}{\sqrt{N}} \sum_k e^{-ik(n+7/12-m/6)} a_{mk}, \end{aligned} \qquad \text{(A3)}$$

where $l = 1, 2, 3$ and $m = 4, 5, 6$. The Hamiltonian, up to the order of $O(S)$, takes the form of

$$H = E_0 + \sum_k \sum_{i=1}^{6} (\omega_i a_{ik}^{+} a_{ik} + \gamma_i a_{ik} a_{i+1k}^{+} + \gamma_i^{*} a_{ik}^{+} a_{i+1k}),$$

where $a_{7k} = a_{1k}$, $E_0 = -2NS^2(J_{AF} - 2J_F)$, $\omega_{1,3,4,6} = S(J_{AF} - J_F) + \mu$, $\omega_{2,5} = -2SJ_F + \mu$, $\gamma_{1,2} = SJ_F e^{-i\frac{k}{6}}$, $\gamma_3 = SJ_{AF} e^{-i\frac{k}{6}}$, $\gamma_{4,5} = SJ_F e^{i\frac{k}{6}}$, and $\gamma_6 = SJ_{AF} e^{i\frac{k}{6}}$. Via the Bogoliubov transformation

$$\begin{aligned} a_{ik} &= u_{i1}(k)\alpha_{1k} + u_{i2}(k)\alpha_{2k} + u_{i3}(k)\alpha_{3k} \\ &\quad + u_{i4}(k)\alpha_{4k}^{+} + u_{i5}(k)\alpha_{5k}^{+} + u_{i6}(k)\alpha_{6k}^{+}, \\ a_{jk}^{+} &= u_{j1}(k)\alpha_{1k} + u_{j2}(k)\alpha_{2k} + u_{j3}(k)\alpha_{3k} \\ &\quad + u_{j4}(k)\alpha_{4k}^{+} + u_{j5}(k)\alpha_{5k}^{+} + u_{j6}(k)\alpha_{6k}^{+}, \end{aligned} \qquad \text{(A4)}$$

where $i = 1, 2, 3$ and $j = 4, 5, 6$, the Hamiltonian can be diagonalized as

$$H = E_g + \sum_k \sum_{i=1}^{6} \sigma_i E_{ik} \alpha_{ik}^{+} \alpha_{ik},$$

where $\sigma_i = +$ for $i = 1, 2, 3$ and $-$ for $i = 4, 5, 6$, and $E_g = E_0 + \sum\limits_k [\sum\limits_{i=1}^{3} \omega_i (\sum\limits_{j=4}^{6} |u_{ij}|^2) + \sum\limits_{i=4}^{6} \omega_i (\sum\limits_{j=1}^{3} (|u_{ij}|^2)]$. The coefficients of the Bogoliubov transformation can be found through equations of motion $i\hbar\dot{a}_{ik} = [a_{ik}, H]$:

$$\begin{pmatrix} \omega_1 & \gamma_1^{*} & 0 & 0 & 0 & \gamma_6^{*} \\ \gamma_1 & \omega_2 & \gamma_2^{*} & 0 & 0 & 0 \\ 0 & \gamma_2 & \omega_3 & \gamma_3^{*} & 0 & 0 \\ 0 & 0 & -\gamma_3 & -\omega_4 & -\gamma_4 & 0 \\ 0 & 0 & 0 & -\gamma_4^{*} & -\omega_5 & -\gamma_5 \\ -\gamma_6 & 0 & 0 & 0 & -\gamma_5^{*} & -\omega_6 \end{pmatrix} \begin{pmatrix} u_{1i} \\ u_{2i} \\ u_{3i} \\ u_{4i} \\ u_{5i} \\ u_{6i} \end{pmatrix} = E_{ik} \begin{pmatrix} u_{1i} \\ u_{2i} \\ u_{3i} \\ u_{4i} \\ u_{5i} \\ u_{6i} \end{pmatrix}.$$

For a given k and μ, the eigenvalues E_{ik} and eigenvectors $(u_{1i}, ..., u_{6i})$ can be numerically calculated by the driver *ZGEEV.f* of the *LAPACK*, which is available on the website[24].

At finite temperature, the Lagrange multiplier $\mu(T)$ is determined through the constraint (A2):

$$\begin{aligned} 6NS &= \sum_k \sum_{j=1}^{6} n_{jk}, \\ n_{lk} &= \sum_{i=1}^{3} |u_{li}|^2 \tilde{n}_{ik} + \sum_{i=4}^{6} |u_{li}|^2 (1 + \tilde{n}_{ik}), \\ n_{mk} &= \sum_{i=1}^{3} |u_{mi}|^2 (1 + \tilde{n}_{ik}) + \sum_{i=4}^{6} |u_{mi}|^2 \tilde{n}_{ik}, \end{aligned} \qquad \text{(A5)}$$

where $l = 1, 2, 3$, $m = 4, 5, 6$, and $n_{jk} = \langle a_{jk}^{+} a_{jk} \rangle_T$. Defining $\tilde{n}_{ik} \equiv \langle \alpha_{ik}^{+} \alpha_{ik} \rangle_T$, the spin-wave distribution function, we have $\tilde{n}_{ik} = [e^{\sigma_i E_{ik}/T} - 1]^{-1}$ with $\sigma_i = +$ for $i = 1, 2, 3$ and $-$ for $i = 4, 5, 6$.

The internal energy and the magnetic susceptibility can be expressed as [17]

$$\begin{aligned} E &= E_g + \sum_k \sum_{i=1}^{6} \sigma_i E_{ik} \tilde{n}_{ik}, \\ \chi &= \frac{1}{3T} \sum_k \sum_{i=1}^{6} \tilde{n}_{ik} (\tilde{n}_{ik} + 1), \end{aligned}$$

where $\sigma_i = +$ for $i = 1, 2, 3$ and $-$ for $i = 4, 5, 6$. E_{ik}, χ and C within the LMSW framework can be thus calculated numerically, as shown in Figs.10.

For the PIMSW method, the HP transformation is treated, up to the order of O(S^0), such that

$$S_{1n}^{+} S_{2n}^{-} \simeq 2S a_{1n} a_{2n}^{+} - \frac{1}{2} a_{1n}^{+} a_{1n} a_{1n} a_{2n}^{+} - \frac{1}{2} a_{1n} a_{2n}^{+} a_{2n}^{+} a_{2n}.$$

The interactions may be handled in the perturbational way:

$$\begin{aligned} a_{1n}^{+} a_{1n} a_{1n} a_{2n}^{+} &\simeq 2\langle a_{1n}^{+} a_{1n} \rangle_0 a_{1n} a_{2n}^{+} + 2\langle a_{1n} a_{2n}^{+} \rangle_0 a_{1n}^{+} a_{1n}, \\ a_{1n} a_{2n}^{+} a_{2n}^{+} a_{2n} &\simeq 2\langle a_{1n} a_{2n}^{+} \rangle_0 a_{2n}^{+} a_{2n} + 2\langle a_{2n}^{+} a_{2n} \rangle_0 a_{1n} a_{2n}^{+}. \end{aligned}$$

Define $\langle a_{1n}^{+} a_{1n} \rangle_0 \equiv C_{11}$, $\langle a_{2n}^{+} a_{2n} \rangle_0 \equiv C_{22}$ and $\langle a_{1n} a_{2n}^{+} \rangle_0 \equiv C_{12}$. We obtain

$$\begin{aligned} C_{11} &= \tfrac{1}{N} \sum_k \langle a_{1k}^{+} a_{1k} \rangle_0 = \tfrac{1}{N} \sum_k (|u_{14}|^2 + |u_{15}|^2 + |u_{16}|^2), \\ C_{22} &= \tfrac{1}{N} \sum_k \langle a_{2k}^{+} a_{2k} \rangle_0 = \tfrac{1}{N} \sum_k (|u_{24}|^2 + |u_{25}|^2 + |u_{26}|^2), \\ C_{12} &= \tfrac{1}{N} \sum_k \langle a_{1k} a_{2k}^{+} \rangle_0 = \tfrac{1}{N} \sum_k e^{-i\frac{k}{6}} (u_{11} u_{21}^{*} + u_{12} u_{22}^{*} + u_{13} u_{23}^{*}), \end{aligned}$$

and

$$\begin{aligned} & \sum_n a_{1n}^{+} a_{1n} a_{1n} a_{2n}^{+} = \sum_k 2(C_{11} a_{1k} a_{2k}^{+} e^{-i\frac{k}{6}} + C_{12} a_{1k}^{+} a_{1k}) \\ = & \sum_k \sum_{i=1}^{6} (2C_{11} e^{-i\frac{k}{6}} u_{1i} u_{2i}^{*} + 2C_{12} |u_{1i}|^2) \alpha_{ik}^{+} \alpha_{ik}, \\ & \sum_n a_{1n} a_{2n}^{+} a_{2n}^{+} a_{2n} = \sum_k 2(C_{12} a_{2k}^{+} a_{2k} + C_{22} a_{1k} a_{2k}^{+} e^{-i\frac{k}{6}}) \\ = & \sum_k \sum_{i=1}^{6} (2C_{22} e^{-i\frac{k}{6}} u_{1i} u_{2i}^{*} + 2C_{12} |u_{2i}|^2) \alpha_{ik}^{+} \alpha_{ik}, \end{aligned} \qquad \text{(A6)}$$

where (...) in (A6) is the up-to-$O(S^0)$ correction to E_{ik} from the term $\langle S_{1n}^{+} S_{2n}^{-} \rangle$, and the other terms have similar contributions to E_{ik}. The only difference between LMSW and PIMSW is E_{ik}, say, the former is treated up to O(S^1), while the latter up to O(S^0). Accordingly, E_{ik}, χ and C within the PIMSW scheme can thus be calculated numerically, as shown in Figs.10.

Acknowledgments

The authors are grateful to H. F. Mu, X. Y. Wang, Q. B. Yan and Q. R. Zheng for helpful discussion and assistance. This work is supported in part by the National Science Foundation of China (Grant Nos. 90403036, 20490210, 10247002).

[] *Corresponding author. E-mail: gsu@gucas.ac.cn.

- [1] H. Manaka, I. Yamada and K. Yamaguchi, J. Phys. Soc. Japan **66**, 564 (1997); H. Manaka and I. Yamada, J. Magn. Magn. Mater. **177**, 681 (1998).
- [2] K. Hida, J. Phys. Soc. Japan **63**, 2359 (1994); M. Oshikawa, M. Yamanaka and I. Affleck, Phys. Rev. Lett. **78**, 1984 (1997).
- [3] J. C. Livermore, R. D. Willett, R. M. Gaura and C. P. Landee, Inorg. Chem. **21**, 1403 (1982); Y. Ajiro, T. Asano, T. Inami, H. Aruga-Katori and T. Goto, J. Phys. Soc. Japan **63**, 859 (1994); T. Toto, Y. Ajiro, T. Asano, T. Inami and H. Aruga-Katori, Physica B **216**, 294 (1996).
- [4] A. Kitazawa and K. Okamoto, J. Phys.: Condens Matter **11**, 9765 (1999).
- [5] M. A. M. Abu-Youssef, M. Drillon, A. Escuer, M. A. S. Goher. F. A. Mautner and R. Vicente, Inorg. Chem. **39**, 5022 (2000).
- [6] S. Martin, M. G. Barandika, L. Lezama, J. L. Pizarro, Z. E. Eerna, J. I. R. Larramendi, M. I. Arriortua, T. Rojo and R. Cortes, Inorg. Chem. **40**, 4109 (2001).
- [7] A. K. Ghosh, D. Ghoshal, E. Zangrando, J. Ribas and N. Ray Chaudhuri, Inorg. Chem. **44**, 1786 (2005).
- [8] A. Escuer, R. Vicente, M. S. El Fallah, M. A. S. Goher and F. A. Mautner, Inorg. Chem. **37**, 4466 (1998).
- [9] M. Hagiwara, Y. Narumi, K. Minami and K. Kindo, Physica B **294**, 30 (2001); M. Hagiwara, Y. Narumi, K. Minami, K. Kindo, H. Kitazawa, H. Suzuki, N. Tsujii and H. Abe, J. Phys. Soc. Japan **72**, 943 (2003).
- [10] J. Strecka, M. Jascur, M. Hagiwara, Y. Narumi, K. Kindo and K. Minami, Phys. Rev. B **72**, 022459 (2005).
- [11] H. T. Lu, Y. H. Su, L. Q. Sun, J. Chang, C. S. Liu, H. G. Luo and T. Xiang, Phys. Rev. B **71**, 144426 (2005).
- [12] B. Gu, G. Su and S. Gao, J. Phys.: Condens. Matter **17**, 6081 (2005).
- [13] R. J. Bursill. T. Xiang and G. A. Gehring, J. Phys.: Condens. Matter **8**, L583 (1996); X. Wang and T. Xiang, Phys. Rev. B **56**, 56 (1997).
- [14] T. Xiang and X. Wang, *Density-Matrix Renormalization*, Lecture Notes in Physics, Vol. 528, edited by I. Peschel, X. Wang, M. Kaulke and K. Hallberg (Springer-Verlag, New York, 1999); U. Schollwock, Rev. Mod. Phys. **77**, 259 (2005).
- [15] P. Mohn, *Magnetism in the Solid State: An Introduction*, Springer Series in Solid-State Sciences, Vol. 134 (Springer-Verlag, Berlin, 2003).
- [16] M. Takahashi and M. Yamada, J. Phys. Soc. Japan **54**, 2808 (1985); M. Yamada and M. Takahashi, J. Phys. Soc. Japan **55**, 2024 (1986).
- [17] M. Takahashi, Prog. Theor. Phys. Suppl. **87**, 233 (1986)
- [18] T. Nakanishi and S. Yamamoto, Phys. Rev. B. **65**, 214418 (2002).
- [19] S. Yamamoto, S. Brehmer and H. J. Mikeska, Phys. Rev. B. **57**, 13610 (1998).
- [20] K. Maisinger, U. Schollwock, S. Brehmer, H. J. Mikeska and S. Yamamoto, Phys. Rev. B. **58**, R5908 (1998).
- [21] S. Yamamoto, Phys. Rev. B **69**, 064426 (2004).
- [22] S. Yamamoto and K. Funase, Low Temp. Phys. **31**, 740 (2005).
- [23] A. S. Ovchinnikov, I. G. Bostrem, V. E. Sintsyn, A. S. Boyarchenkov, N. B. Baranov and K. Inoue, J. Phys.: Condens. Matter **14**, 8067 (2002).
- [24] http://www.netlib.org/lapack/.